4. CELL PROLIFERATION INFLUENCED BY MATRIX COMPLIANCE OF GELATIN GRAFTED POLY(D,L-LACTIDE) THREE DIMENSIONAL SCAFFOLDS

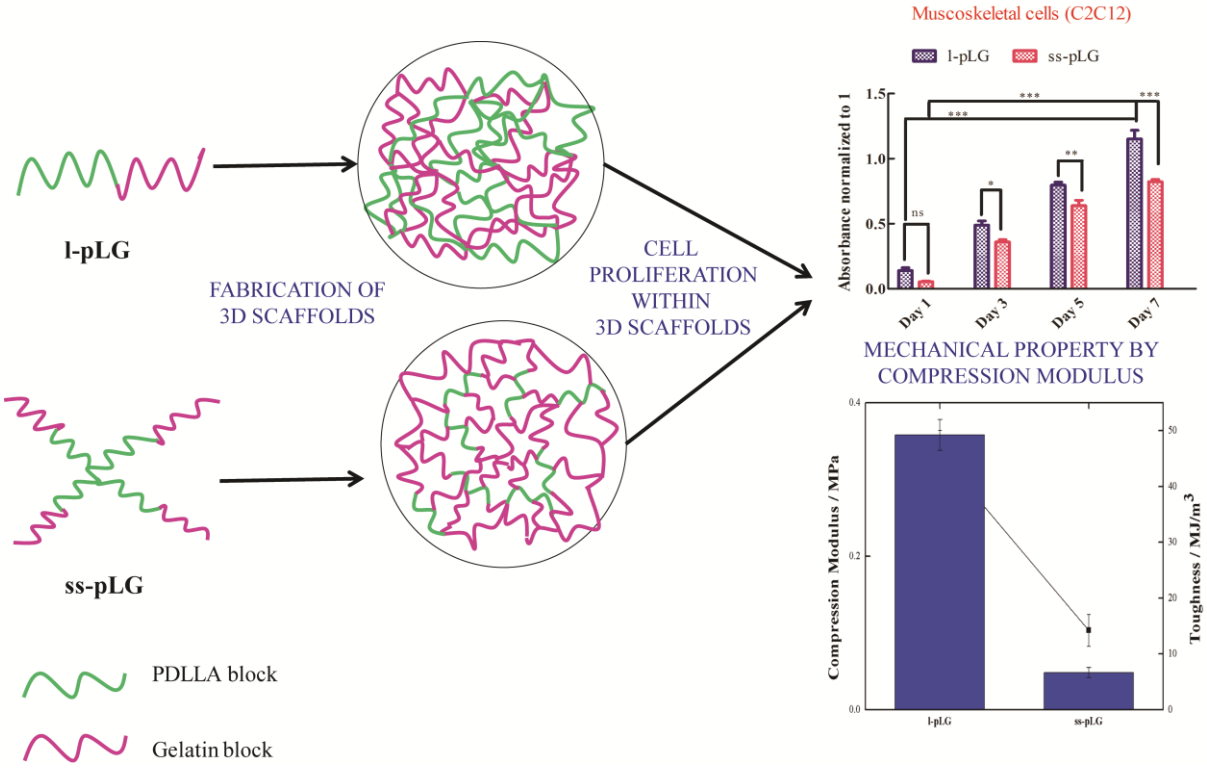

This chapter describes about tailoring the mechanical strength by variable grafting of gelatine to PDLLA backbone and their respective cell proliferation potential.

4.1. OVERVIEW

The, critical parameters of tissue engineering scaffolds are wettability, surface roughness and structural composition of the material. [122-126] However, studies on improvements on mechanical properties of the scaffolds and their relevance in recreating the desired tissue structures are limited because of the lack of understanding in controlling of cell adhesion and proliferation by the mechanical properties of 3D scaffolds. [127-130] In addition, identification of an appropriate approach that simultaneously improves both the mechanical and biological performance of tissue engineering scaffolds remains a significant challenge. The mechanical property of PLA can be modulated by molecular weight of the polymer,[10] branching the polymer,[10] crosslinking, [131, 132] and using fillers like hydroxyapatite (HA),[133] and bioglass[134]. However, modulating the mechanical property of PLA together with efficient cell proliferation with distinct properties has not been reported yet.

Herein, we synthesized linear PDLLA-b-gelatin (l-pLG) and demonstrated the mechanical property of l-pLG and the preciously synthesized ss-pLG, 3D scaffolds. To establish the comparative study for the tissue-level compatibility of 1-pLG and ss-pLG, we cultured three different cell types such as fibroblasts (L929), muscoskeletal cells (C2C12) and preosteoblasts (MG-63) that originally belong to the distinct tissue lineages and differ in their respective matrix stiffness.

4.2. RESULTS AND DISCUSSION

4.2.1. Synthesis and characterization of l-pLG

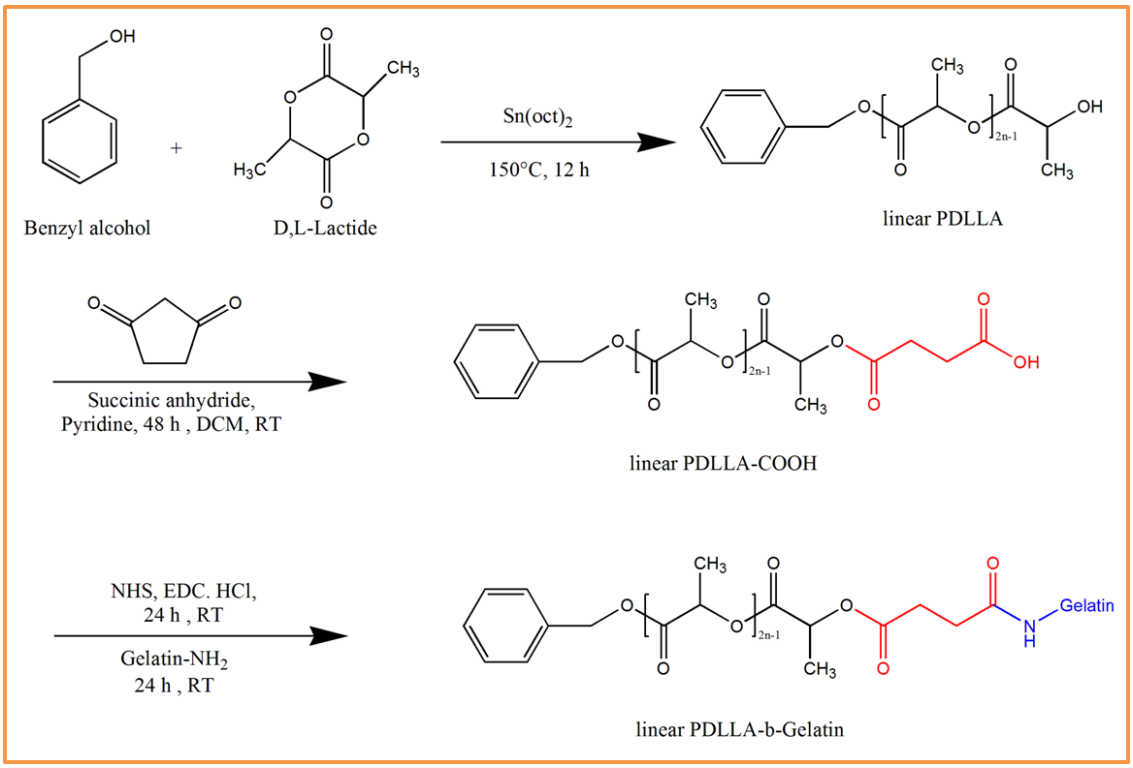

Figure 4.1. Reaction scheme for synthesis of l-pLG by ROP and carbodimide mediated end functionalization chemistry.

The linear gelatin grafted PDLLA (l-pLG) was synthesized as explained in **Figure 4.1**. l-PDLLA was synthesized by bulk polymerization of D,L-Lactide at 150 °C using benzyl alcohol as initiator and $Sn(Oct)_2$ as catalyst, while maintaining the molar feed ratio of D,L-Lactide to benzyl alcohol at 693.3. [21] M_n (NMR) and conversion (NMR) was found to be 2,06,010 g mol^{-1} and 98.8% respectively (**Figure 4.2A(**a) & **Table 4.1**). To graft gelatin into the backbone of l-PDLLA, carboxyl terminated l-PDLLA was first synthesized. The disappearance of end terminal methine proton of l-PDLLA at 4.36 ppm (e) and the appearance of new peak at 3.67 ppm (*h+i*), which arises from the

methylene protons of succinic anhydride confirms successful ring opening reaction (**Figure 4.2**A(b)).

Table 4.1 GPC Characteristic data of linear PDLLA

Sample	**Conversion (%)[a]**	M_n**(NMR)[b]**	M_n**(GPC)[c]**	M_n/M_w
l-PDLLA	98.8	206010	394000	2.1

[a] Conversion was determined by comparing the peak area of the residual poly(D,L-Lactide) ~ 5.1-5.2 and monomer D,L-Lactide ~ 5.3 ppm using ^{1}H NMR

[b] Determined from ^{1}H NMR by comparing the methylene proton of benzyl alcohol and methine proton of l-PDLLA at ~ 7.3 and ~ 5.2 ppm

[c] Determined by GPC (DMF, 0.5 mL/min, 40 ºC) calibrated against PMMA standards

Further, the end terminal –COOH group was activated by EDC.HCl and NHS followed by coupling with gelatin. Gelatin grafting to l-PDLLA backbone was confirmed by ^{1}H NMR (Figure S1), that revealed both the characteristic peaks of gelatine and characteristic peaks of l-PDLLA at 5.1-5.2 and 1.46 ppm corresponding to the backbone methine and pendent methyl protons, respectively (**Figure 4.2**A(d)). Gravimetric yield of the synthesized l-pLG was determined as 85.87%. Thus, we could infer that approximately 70.17% of gelatin was grafted into the backbone l-PDLLA.

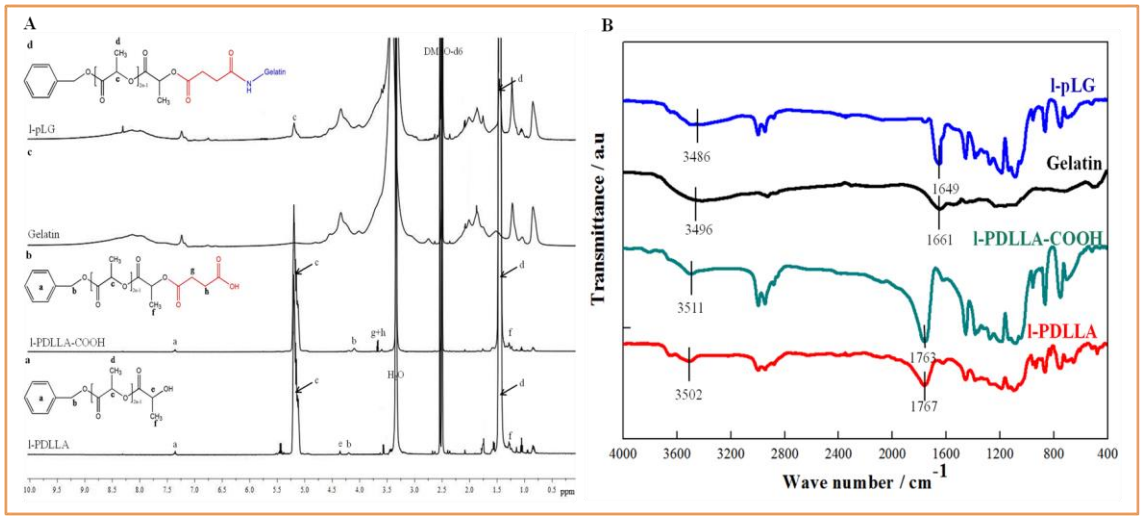

Figure 4.2. Characterization of l-pLG: (A) ^{1}H NMR spectra of linear polymers namely l-PDLLA-COOH, Gelatin and l-pLG (B) FTIR spectra of the respective series of linear polymers.

Figure 4.2B shows the respective FTIR spectra of l-PDLLA-COOH, gelatin and l-pLG. l-PDLLA showed its characteristic distinct C=O stretching peak at 1767 cm^{-1} and pure gelatin showed its characteristic distinct amide stretches peaks at 1661 and 3496 cm^{-1}. When l-PDLLA-OH opened succinic anhydride ring, a shifting was observed from 1767 to 1763 cm^{-1}. After grafting of gelatin into l-PDLLA back bone, amide stretching peaks from 1661 and 3496 cm^{-1} shifted to the lower frequencies 1649 and 3486 cm^{-1}, respectively, whereas in case of ss-pLG, the shift in amide stretching was observed at 1627 and 3284 cm^{-1}[122]. This observation suggests that $–NH_2$ group of gelatin has successfully coupled with the -COOH group of l-PDLLA.

4.2.1.1. Crystallinity and Thermal Properties of Polymers

X-ray diffraction pattern of gelatin, l-PDLLA and l-pLG is shown in **Figure 4.3**A. No sharp peak was observed in XRD pattern of gelatin and unmodified polymer l-PDLLA, which clearly supported their amorphous nature. Importantly, there was no change in

crystallinity observed even after gelatin grafting into the l-PDLLA backbone. However, a significant shift in the peak was observed as in l-pLG [122] which could be likely due to the gelatin grafting into l-PDLLA. XPS confirmed the presence of gelatin in the l-pLG films as the observation of nitrogen peak and the shift in the binding energy compared to gelatin, whereas unmodified l-PDLLA did not show any peak corresponding to the nitrogen in XPS spectrum (data not shown) (**Figure 4.3**B) [63].

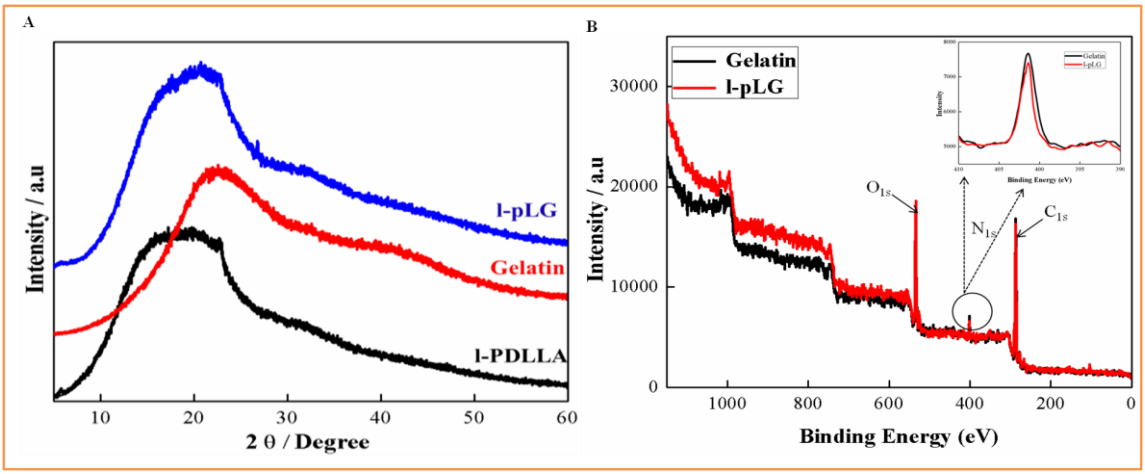

Figure 4.3. Crystallinity of l-pLG. (A) XRD profile of linear unmodified and gelatin grafted polymers (B) XPS spectra of l-pLG and gelatin..

Figure 4.4A shows thermal degradation profile of l-PDLLA, gelatin, and l-pLG. Gelatin showed highest T_{max} (**Table 4.2**). T_{max} of l-PDLLA and l-pLG was observed as 291 and 365 °C, respectively, indicating that improved thermal property was exhibited on l-pLG compared to unmodified l-PDLLA. This improved thermal behaviour may be attributed to the grafting of gelatin onto the l-PDLLA back bone. Moreover, two distinct degradation peaks were observed for l-pLG, possibly due to PDLLA and gelatin block.

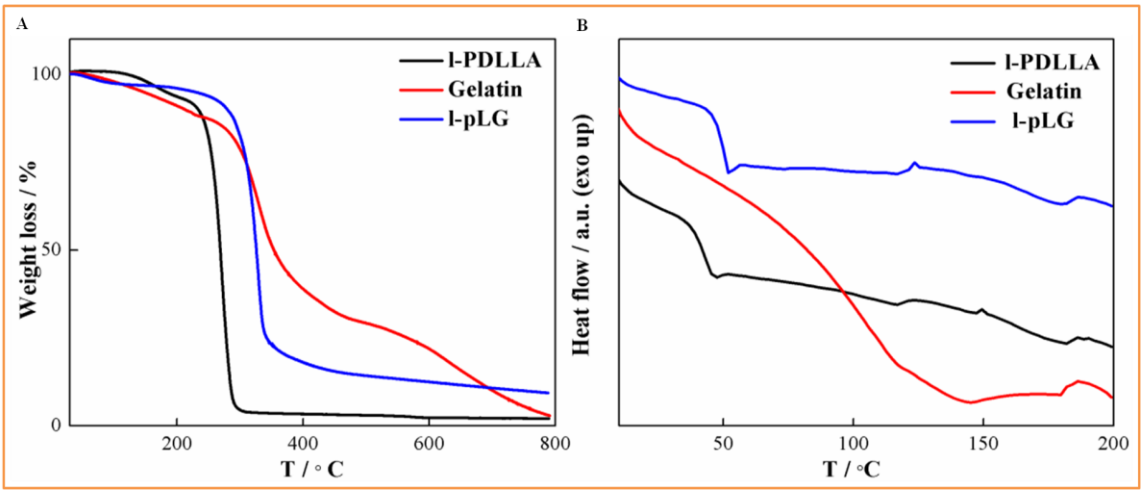

Figure 4.4. Thermal properties of l-pLG. (A) TGA thermograms of linear unmodified and gelatin grafted polymers. (B) DSC thermograms of linear unmodified and gelatin grafted polymers.

Table 4.2 Thermal degradation properties of l-PDLLA, Gelatin and l-pLG determined by TGA

S.No	Sample(s)	T_{onset} (°C)	T_{max} (°C)
1.	l-PDLLA	225	291
2.	Gelatin	285	457
3.	l-pLG	271	354

DSC analyses of l-PDLLA, gelatin and l-pLG are demonstrated in **Figure 4.4**B. T_gs were observed at 47.63, 142.9 and 51.56 °C for l-PDLLA, gelatin and l-pLG, respectively [31, 32]. l-PDLLA showed an exotherm peak at 148 °C due to recrystalization behaviour of the amorphous PDLLA at that particular temperature

[135]. A clear shift of T_g was observed from 47.63 to 51.56 °C for l-pLG, most likely due to the grafting of gelatin into PDLLA.

4.2.2. Characterization of 3D scaffolds

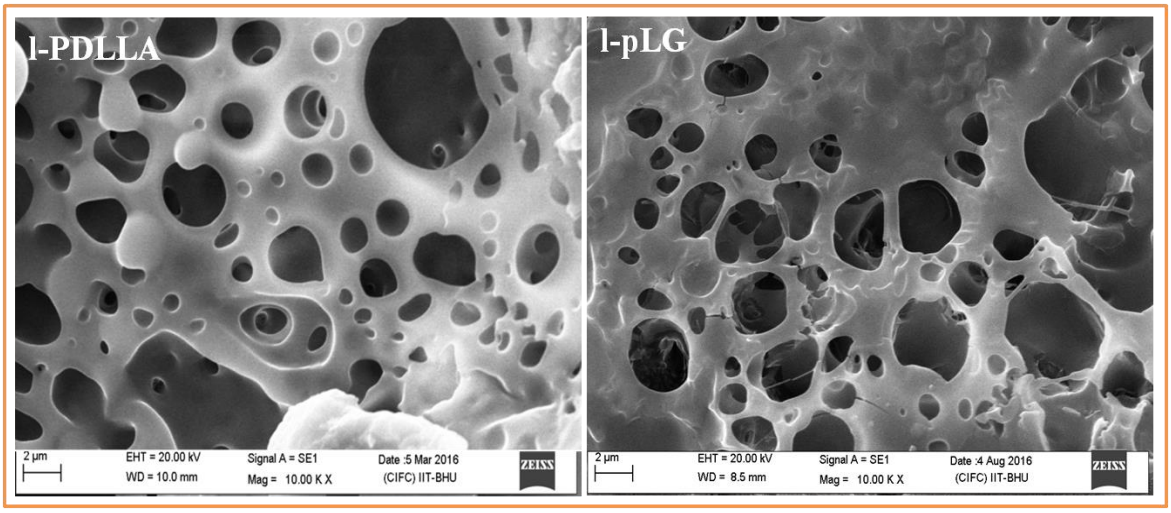

Figure 4.5. SEM Morphology of 3D scaffolds fabricated from 12 % of polymer in DMSO, through freeze drying.

Table 4.3. Pore size of fabricated 3D scaffolds

S.No	Sample(s)	Pore size (µm)
1.	l-PDLLA	29.23±13.9
2.	l-pLG	35.32 ± 8.75

3D porous scaffolds are widely fabricated by phase separation followed by solvent evaporation [66, 110]. SEM images (**Figure 4.5**) show the representative surface morphology of unmodified l-PDLLA and gelatin grafted l-pLG scaffolds. The porous interconnected network structure of lyophilized l-pLG scaffold was distinctly different

from its unmodified l-PDLLA owing to the chemical modification in the polymer backbone as we observed in ss-pLG[122]. The mean pore diameter of l-PDLLA and l-pLG was estimated as 29.23±13.9 and 38.7±15.39 μm, respectively (**Table 4.3**), On the other hand, the percentage of porosity of l-PDLLA and l-pLG were found as 65.3±4.6 and 68.1±3.9%, respectively. These results indicate that gelatin grafting increases the pore size of the 3D scaffolds because of the mobility of gelatin into the l-PDLLA back bone.

4.2.3. *In vitro* biomolecule release and release kinetics

An anti-cancerous drug docetaxel (DTX) was chosen as the model biomolecule and we studied the drug release kinetics using UV-Visble spectrophotometer. **Figure 4.6** shows the characteristic release profile of DTX from modified and unmodified polymeric 3D scaffolds. Short time and immediate release of DTX was found from the gelatin modified hydrophilic polymeric scaffolds (l-pLG and ss-pLG). 63% and 65% of initial burst release of DTX after 1 h and followed by 85% release was observed after 3 h and 5 h of incubation from l-PG and ss-PG scaffolds, respectively (**Figure 4.6**A). On the other hand, hydrophobic polymeric scaffolds showed sustained release of DTX from its matrix, where 45 % and 62 % of DTX was released from l-PDLLA and ss-PDLLA scaffolds respectively after 48 h (**Figure 4.6**B). Sustained release of DTX from unmodified scaffolds may be due to the strong hydrophobic interaction between the drug and polymers (l-PDLLA and ss-PDLLA). Hydrophobic unmodified polymers controlled the drug release whereas super hydrophilic polymer ss-pLG showed higher drug release in short time. The half-lives of most growth factors are very short, so an optimal growth factor-delivering scaffold should possess “burst release” it is essential

for the bioactive scaffolds to maintain a desired temperospatial growth factor concentration to direct tissue regeneration[136]. It has also been shown at the beginning of wound treatment, an initial burst provides immediate relief followed by prolonged release to promote gradual healing.[137] We believe that our strategy can be used for delivering the growth factors at the implantable site or drugs require for wound healing purpose since our modified hydrophilic scaffolds release the DTX in a fast manner.

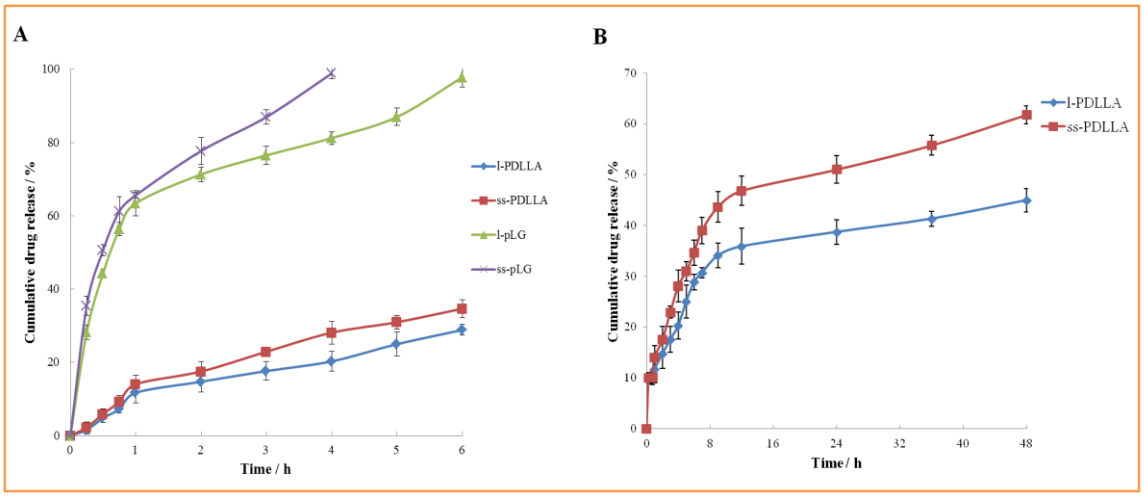

Figure 4.6 . *In vitro* drug (DTX) release profiles from l-PDLLA, ss-PDLLA, l-pLG and ss-pLG scaffolds. (A) DTX release upto 6 h from unmodified and modified scaffolds (B) DTX release upto 48 h from unmodified l-PDLLA and ss-PDLLA scaffolds. . The results presented are mean ± standard deviation (SD) values obtained from three independent experiments.

To understand the DTX release kinetics and mechanism from the hydrophobic and hydrophilic scaffolds, four kinetic models (zero order, first order, Higuchi model and Korsmeyar-Peppas model) were used.[138] The linear correlation coefficient (R^2) values of each model respective to the scaffolds are presented in **Table 4.4**. Zero and first order models were found to be poor fitting to both hydrophobic and hydrophilic scaffold system. Higuchi model kinetics was shown to be the best fit for l-PDLLA and

ss-PDLLA scaffolds (R^2= 0.956 and 0.982 for l-PDLLA and ss-PDLLA respectively). On the other hand, l-pLG and ss-pLG were fit with Korsmeyer- Peppas model (R^2= 0.930 and 0.977 for l-pLG and ss-pLG respectively). The release exponent (n) was calculated by Korsmeyer-Peppas model for l-PDLLA, ss-PDLLA, l-pLG and ss-pLG scaffolds loaded with DTX, was found to be 0.348 and 0.44, 0.333 and 0.346 respectively. Therefore, the mechanism of DTX release form both hydrophobic and hydrophilic scaffolds were found to be Fickian diffusion.

Table 4.4 Correlation coefficient (R^2) and release exponent (n) values of *in vitro* DTX release from l-PDLLA, ss-PDLLA, l-pLG and ss-pLG scaffolds

Model of release kinetics	Correlation co-efficient (R^2) values				Release exponent (n)			
	l-PDLLA	ss-PDLLA	l-pLG	ss-pLG	l-PDLLA	ss-PDLLA	l-pLG	ss-pLG
Zero order	0.911	0.942	0.744	0.763	-	-	-	-
First order	0.932	0.964	0.843	0.666	-	-	-	-
Higuchi Model	0.956	0.982	0.918	0.950	-	-	-	-
Korsmeyer-Peppas model	0.894	0.930	0.930	0.977	0.35	0.44	0.33	0.35

4.2.4. Influence of gelatin grafting in degradation of 3D scaffolds

The stability of 3D scaffolds in biological environment determines the potential of the scaffolds for tissue engineering applications. Our biological system has multiple enzymes in the physiological environment and the degradation kinetics with mixture of enzymes may mimic the bioloigical scenario. Therefore, proteinase K and proteinase K + lysozyme mixture were used to mimic the biological scenarios and degradation kinetics was further studied lasting for 7 days. Proteinase K is known for hydrolysis of the ester bonds[139] and lysozyme is known to hydrolyze the amide group of gelatin [70] and ester groups of PLA [111]. **Figure 4.7**A shows the weight loss profile of l-pLG and ss-pLG scaffolds in proteinase K. After 7 days of incubation, the weight loss of l-pLG and ss-pLG was observed as 39.13±1.73 and 50.38±1.65%, respectively. On the other hand degradation kinetics was also studied in enzyme containing medium,

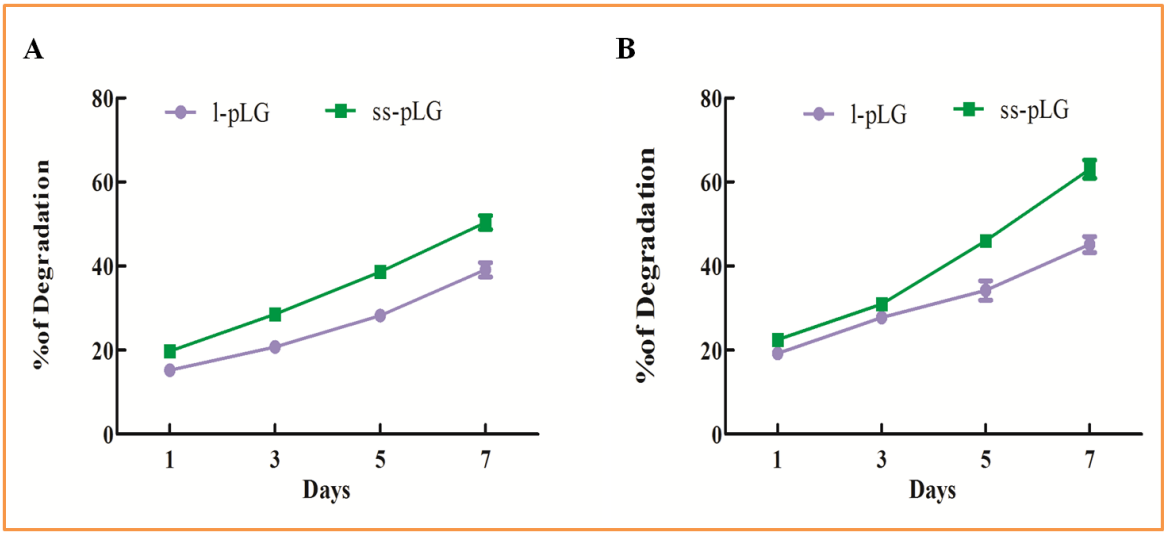

Figure 4.7. Degradation kinetics of 3D scaffolds. Percentage of weight loss of 3D scaffolds after incubation with (A) proteinase K and (B) proteinase K + lysozyme mixture.

Proteinase K is known for hydrolysis of the ester bonds[139] and lysozyme is known to hydrolyze the amide group of gelatin [70] and ester groups of PLA [111]. **Figure 4.7**B

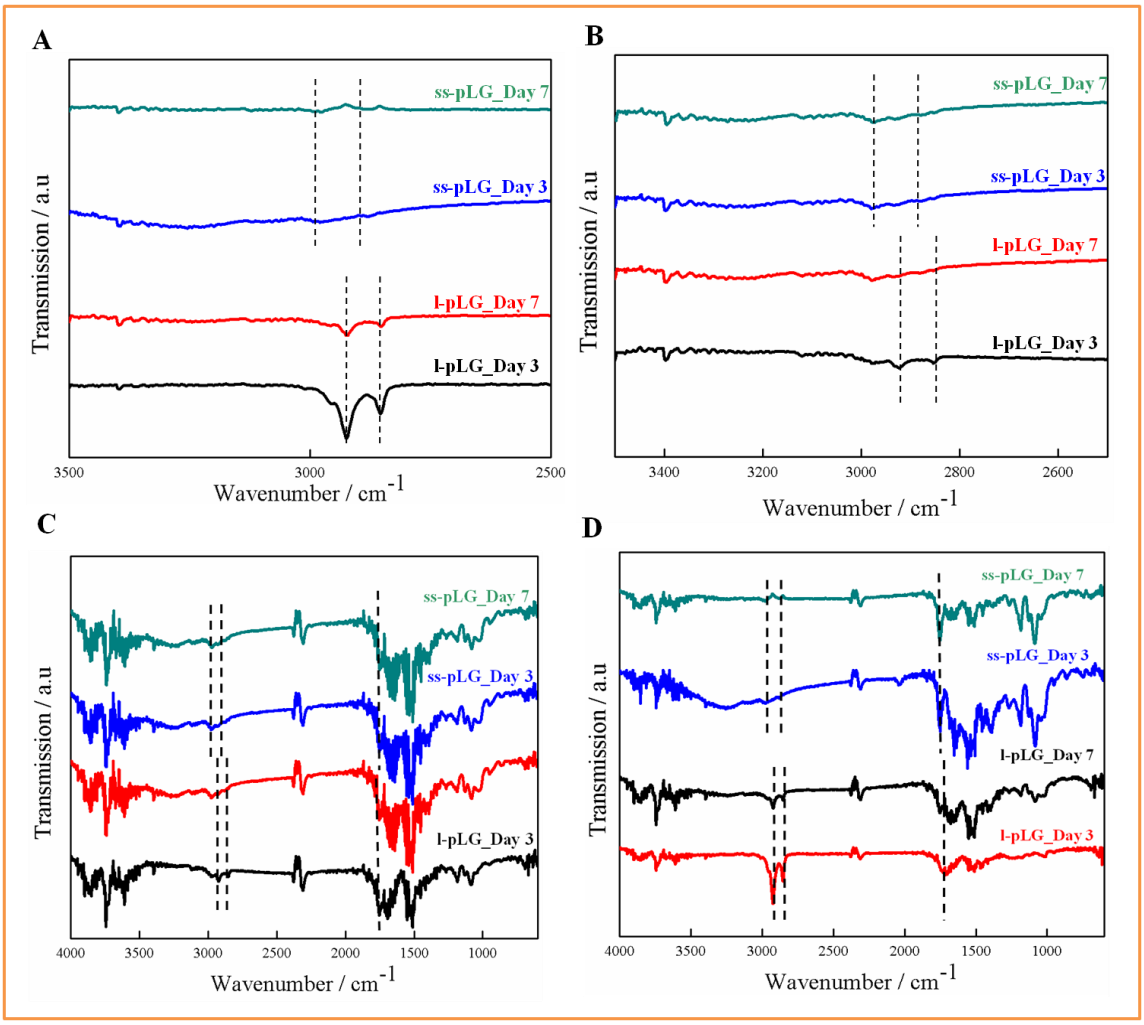

Figure 4.8 Degradation kinetics of 3D scaffolds. FTIR spectrum of 3D scaffolds after incubating in proteinase K (A,C) and proteinase K + Lysozyme mixture (B,D).

shows weight loss profile of scaffolds while incubating in proteinase K+lysozyme mixure containing PBS medium. After 7 days of incubation in proteinase K+lysozyme, it was observed that the weight loss was marginally high incase of ss-pLG (63.06±2.15 %) as compared to l-pLG (45.13±1.88). This higher degradation rate of ss-pLG may be

attributed to the branching of lactide units and the gelatin grafting**. Figure 4.8**A, B shows the FTIR spectrum of scaffolds while incubating in enzyme containing PBS medium. After 7 days of incubation in proteinase K + lysozyme mixture, the intensity of $–CH_2$ was decreased[140], whereas peak of –C=O for PDLLA backbone was shifted in case of both l-pLG and ss-pLG scaffolds and –CONH- stretch around ~1600-17000 cm^{-1} was almost disappeared in ss-pLG scaffolds (**Figure 4.8**C,D). This indicates, ss-pLG scaffolds are more prone to be affected by enzymes compared to l-pLG.

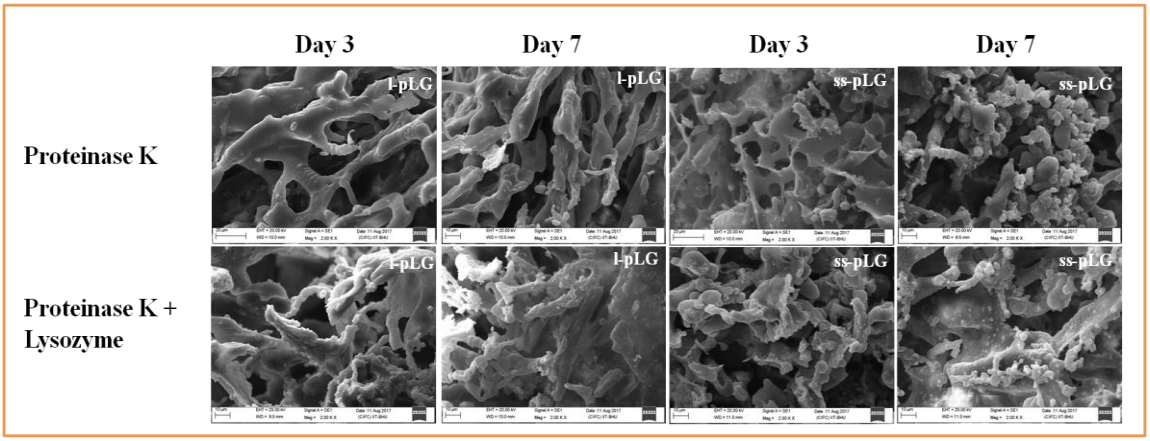

Figure 4.9 SEM morphology of 3D scaffolds after degradation.

SEM images (**Figure 4.9**) demonstrate the time-dependent morphological change of both scaffolds in proteinase K and proteinaseK+lysozyme mixture containing PBS medium. Significant morphological changes were observed after 3 days in both the scaffolds with the disruption of internal geometry and altered surface morphology. A huge disruption of inter-connected structure and changes in surface morphology was seen in ss-pLG after 7 days of incubation in proteinase K + lysozyme mixture, whereas l-pLG scaffold structure was observed less affected. This indicates that scaffolds with larger pore sizes degrade faster as observed in case of ss-pLG, which also complies with

our FTIR observation. Our results are in good agreement with the reports of other authors [67, 112].

4.2.5. Influence of mechanical property of 3D scaffolds in cell proliferation

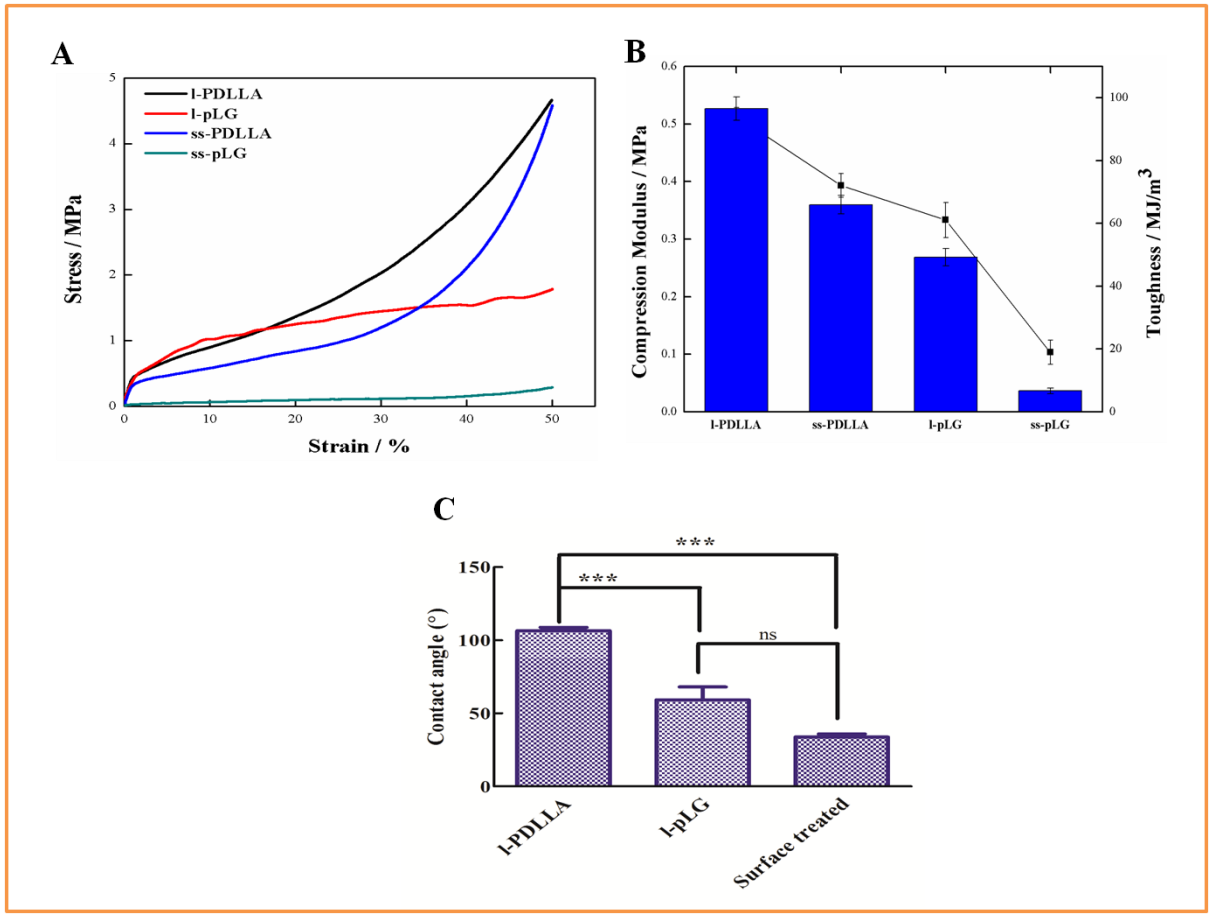

Figure 4.10. Mechanical property of 3D scaffolds with respect to contact angle (A) Stress- Strain curve of the synthesized polymer at 50 % compression (B) Comparison of modulus and toughness of gelatin grafted polymer scaffolds. (C) Water contact angle measurement of polymers compared with surface treated commercial cover glass.

It has been reported that matrix compliance is necessary for the cells to exhibit the appropriate cellular responses [127, 141]. In the view of above facts, strength of the fabricated 3D scaffolds was evaluated by universal testing machine (UTM). The stress versus strain curve of the 3D scaffolds at 50% compression is shown in **Figure**

4.10A,B. Grafting of gelatin into PDLLA backbone significantly reduced the toughness of the scaffolds and in case of ungrafted gelatin, branching of PDLLA also reduced the toughness as observed in published reports[10]. ss-pLG scaffolds showed relatively lower toughness compared to all the evaluated scaffolds. The higher toughness of l-PDLLA suggests that molecules of PDLLA were strongly bound and when the gelatin was grafted into the PDLLA backbone (in the case of l-pLG and ss-pLG), weak interation was observed, since gelatin is hydrophilic in nature (**Figure 4.10**C). This can be clearly observed in l-pLG and ss-pLG scaffolds, where the toughness of l-pLG was

Table 4.5 Mechanical properties of 3D scaffolds from l-pLG and its respective unmodified l-PDLLA by 50 % compression

Sample(s)	**Compression modulus (MPa)**	**Toughness (MJ/m^3)**	**Ultimate strength at 50 % compression (MPa)**
l-PDLLA	0.50	97.65	4.67
ss-PDLLA	0.37	68.48	4.19
l-pLG	0.34	50.05	1.79
ss-pLG	0.12	5.68	0.30

found significantly higher than ss-pLG. The disparity in porosity also could be another reason for the decrease in toughness of l-pLG and ss-pLG scaffolds (**Figure 4.10**B **&**

Table 4.5). Although the modulus of the l-pLG and ss-pLG scaffolds decreased significantly, fracture was not observed till 50% compression. To establish the influence

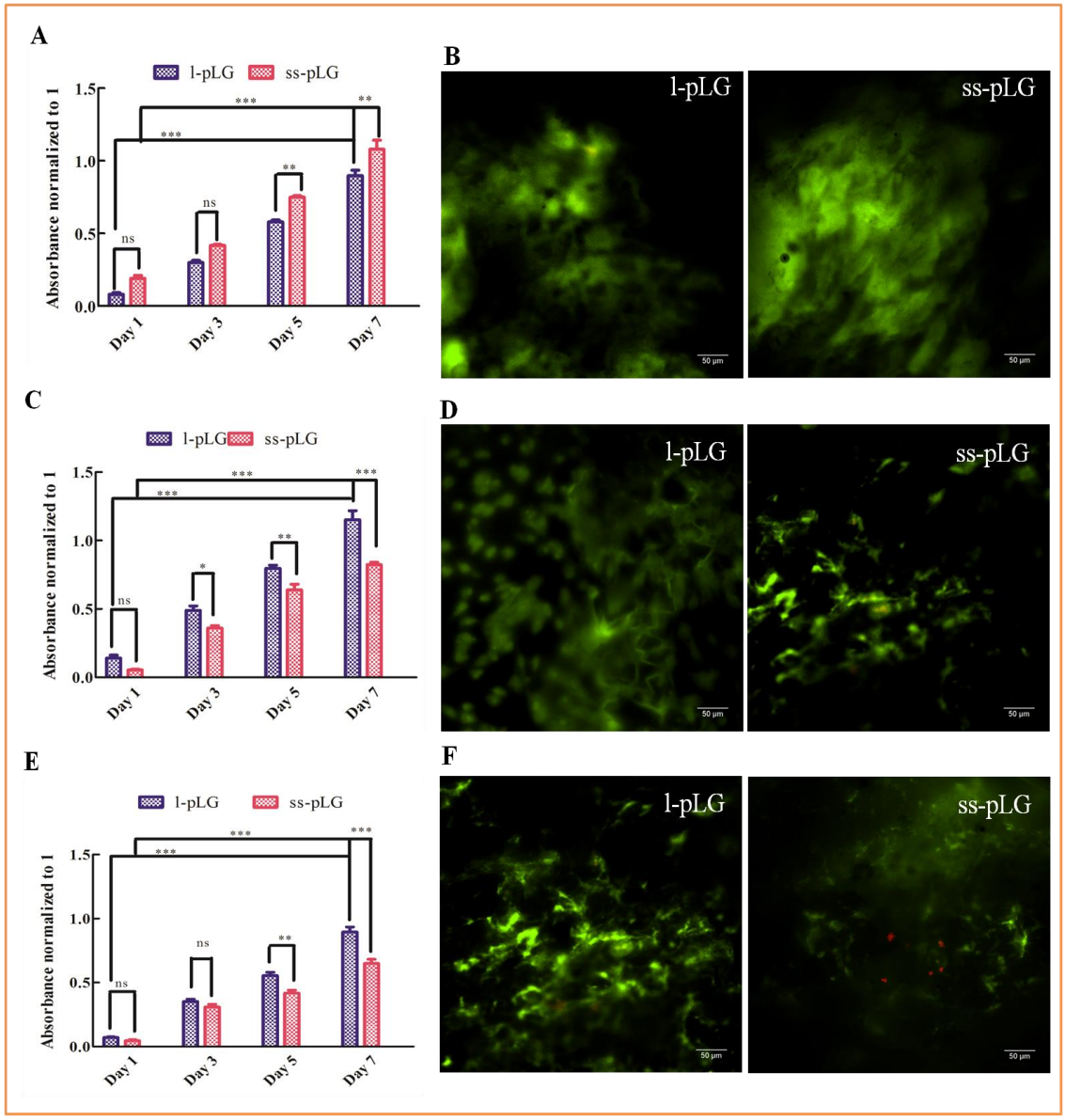

Figure 4.11. Cell Proliferation within 3D scaffolds. Viability of (A) L929, (B) C2C12 and (C) MG-63 cells within the scaffolds assessed by MTT assay. All bars expressed as mean values ± SD (n=3); * p <0.05 , **p<0.001 *** p<0.0001. Qualitative Live/Dead Fluorescence images of L929 (E) C2C12 and (F) MG-63 cells within 3D scaffolds after 3 days of cell seeding using Calcein AM (green) and ethidium homodimer (red).

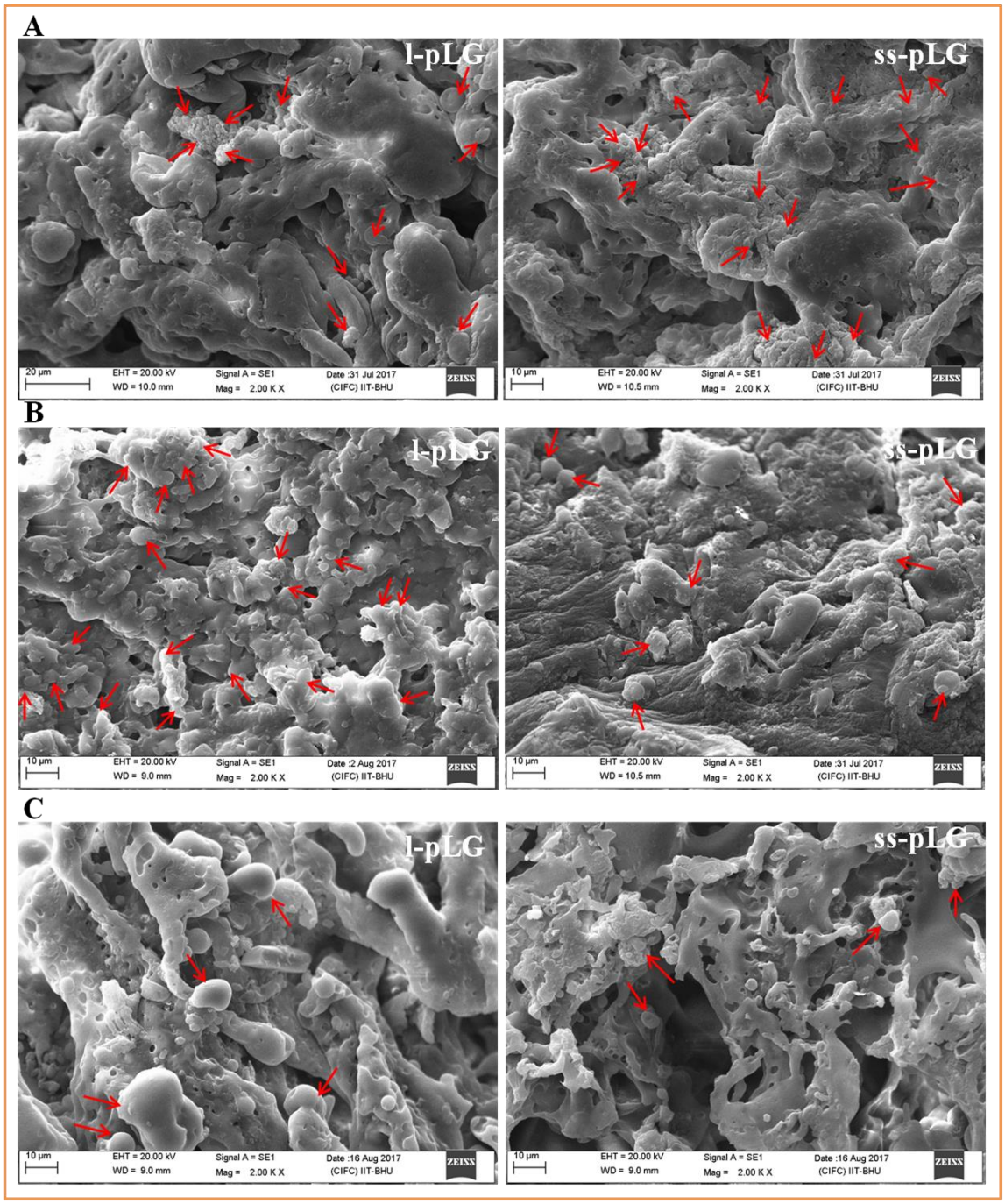

Figure 4.12. Cell Proliferation within 3D scaffolds. SEM micrograms of (G) L929, (H) C2C12 and (I) MG-63 cells seeded scaffolds, after 3 days of seeding. Images are of 2000 X magnified.

of matrix strength on cell proliferation, we chose cells of varying tissue origin such as L929, C2C12 and MG-63 cells which are equivalent to the ultimate strength of

subcutaneous adipose tissue (11.67 kPa),[142] musculoskeletal ligament (1.2-1.8 MPa)[143] and bone (18 GPa)[143]. Viability of the cells grown on modified l-pLG and ss-pLG scaffolds are shown in **Figure 4.11A**,C and E. We observed different rate of proliferation in both the scaffolds. L929 cells grown within both the scaffolds showed a significant increase in cell number till seventh day, whilst rate of proliferation was more on ss-pLG compared to l-pLG scaffolds. On the other hand, C2C12 cells were viable and evenly proliferated on both the scaffolds but the rate of proliferation was more on l-pLG compared to ss-pLG scaffolds. In case of MG-63, rate of cell proliferation was poor on both the scaffolds since the strength of scaffolds was not equivalent to the natural bone tissue. Cell viability was also evaluated by fluorescence microscopy using a live/dead cell staining kit. **Figure 4.11**D,E and F show the viability of L929,C2C12 and MG-63 cells cultured within the scaffolds after 3 days of culture. This study revealed that the number of live cells of L929 were notably more within ss-pLG; C2C12 were considerably better within l-pLG. This qualitative result is in good agreement with the MTT data revealing that cell proliferation was influenced by mechanical strength of the scaffolds.

SEM images of cells seeded scaffolds were acquired to support our quantitative MTT results. **Figure 4.12** shows the typical micrographs of L929,C2C12 and MG-63 cells within scaffolds (which supported efficiently) after 3 days of cell seeding. It was observed that ss-pLG and l-pLG scaffolds efficiently supported L929 and C2C12 cells, respectively. We were also able to see the cells migrated within the pores of the scaffolds. On the other hand L929 and C2C12 cells were adhered well on l-pLG and ss-pLG, respectively, however the cell number was relatively low compared to ss-pLG, l-

pLG and l-pLG scaffolds. In the case of MG-63, cells networking were poor within both the scaffolds. These combined results clearly revealed that l-pLG and ss-pLG scaffolds supported efficient proliferation of C2C12 and L929 cells, respectively. This difference in cellular growth within the scaffolds may be attributed to the stiffness of the scaffolds, where most tissue cells not only adhere but also pull on their microenvironment and thereby respond to its stiffness in ways that relate to tissue elasticity.[127] This result implies that gelatin in PDLLA backbone favoured cellular adhesion followed by cell proliferation; nonetheless due to the difference in stiffness, proliferation of C2C12 and L929 cells was observed significantly more on l-pLG and ss-pLG scaffolds, respectively. Thus, gelatin grafting on PDLLA backbone significantly changes the mechanical strength and provide biochemical and physical cues that considerably support cell proliferation.

4.2.6. Hemocompatability

4.2.6.1. Evaluation of erythrocyte membrane integrity

Blood RBCs are more susceptible to the environment, and therefore get lysed even when they come in contact with water. Hence, the fabricated biomaterials should maintain the integrity and functionality of erythrocytes in the whole blood sample. **Figure 4.13**A shows the hemolysis of the fabricated scaffolds for 1 h and 8 h compared with the control PBS solution. The percentage of hemolysis after 1 h of incubation was found as 2.84±0.35 and 2.63±0.41 for the l-PDLLA and l-pLG scaffolds, respectively, suggesting that scaffolds are hemocompatile since up to 10 % hemolysis is permissible for biomaterials [119]. Furthermore, there was no significant difference ($p>0.05$) was

observed in the levels of hemolysis during the extended period (8 h) in case of l-pLG and l-PDLLA scaffolds with respect to PBS.

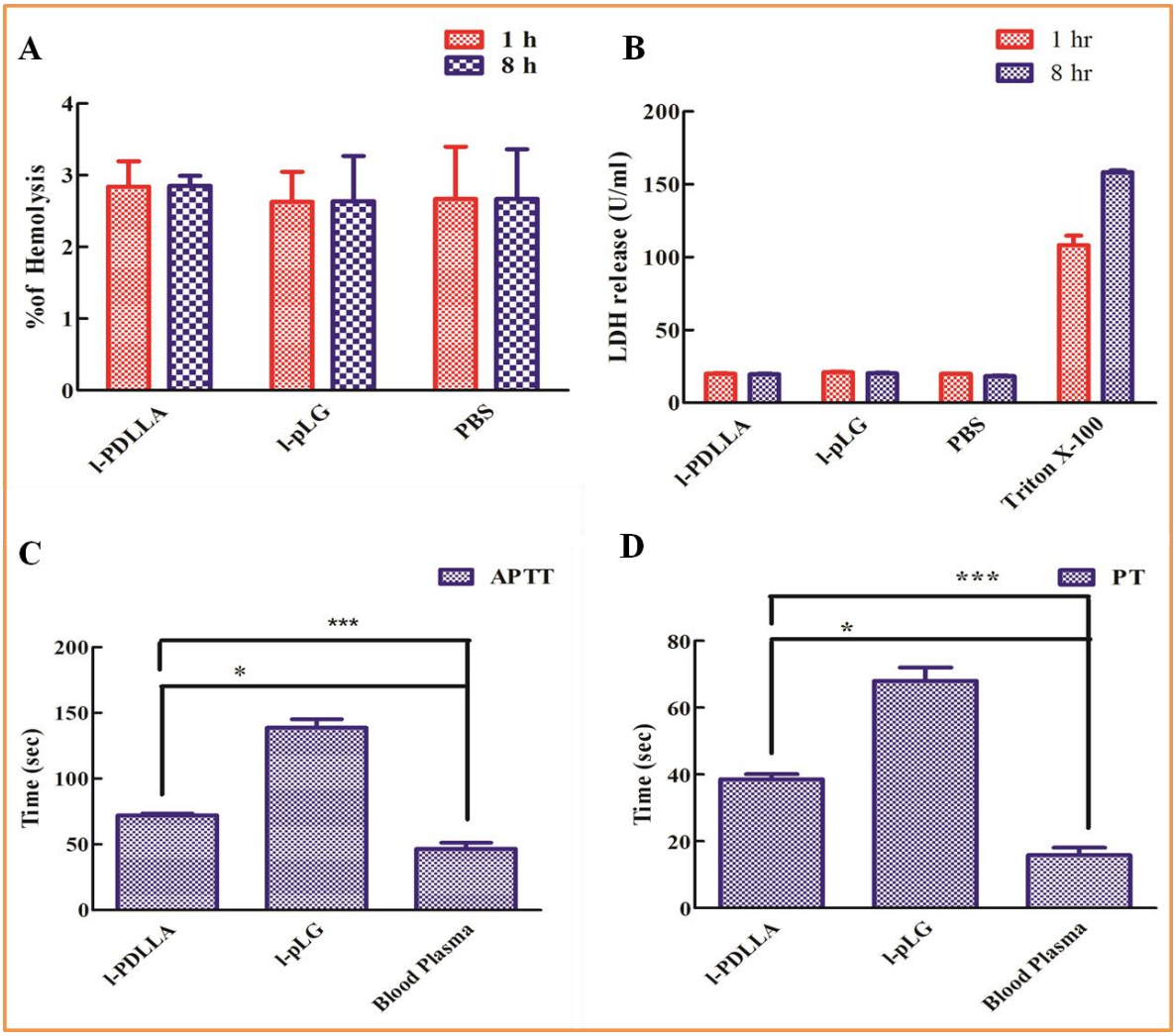

Figure 4.13. Hemocompatability of biomimmetic 3D scaffolds (A) Hemolysis of the scaffolds after 1 h and 8 h; no significant difference were observed in comparison to that of PBS; (B) LDH release assay, compared to 1% Triton X-100 and PBS as positive and negative control. (C) Activated Partial Thromboplastin Time (D) Prothrombin Time. All bars are expressing mean values± SD (n=3); ns- nonsignificant; * $p<0.05$; *** $p<0.0001$

Membrane integrity of erythrocytes when incubated with our fabricated scaffolds was also supported by quantifying the enzyme LDH (**Figure 4.13**B). RBCs suspended in

PBS were used to quantify the LDH released from the cells. At different time intervals, the possible disturbances in membrane integrity of erythrocytes by the scaffolds were observed. Scaffolds incubated with erythrocytes did not show any significant increase ($p>0.05$) in LDH release when compared to PBS (negative control) after 1 h and 8 h interval. These results indicate that the scaffolds maintain the membrane integrity of erythrocytes and did not cause any damage to the cell membrane.

4.2.6.2. Activated Partial Throboplastin Time (APTT) and Prothrombin Time (PT)

APTT and PT are mainly used to examine the intrinsic and extrinsic pathways, respectively. **Figure 4.13**C demonstrates the effects of l-pLG and l-PDLLA scaffolds on APTT in blood plasma. l-pLG scaffolds incubated in blood plasma showed delayed coagulation, as compared to l-PDLLA and control blood plasma.

Figure 4.13D shows the PT when the scaffolds were incubated in blood plasma. Although the trends of PT and APTT were similar, the clotting time was found nearly half of APTT. Albeit most of the hydrophilized surfaces exhibit good hemocompatibility, most of them are not truly anti-thrombogenic but only of anti-thromboadhesive as they curtail or adhesion of platelets and other blood cells instead of prolonging the coagulation time Thus, the combined study of the reported literatures and our observations suggest that the delayed activation of intrinsic and extrinsic blood coagulation pathways was mainly due to the hydrophilic nature of the l-pLG scaffolds [105, 120, 121].

4.3. Conclusion

We have successfully synthesized functional l-pLG and ss-pLG polymers with cell adhesive properties. The synthesis was characterized by ^{1}H NMR and FTIR spectroscopy. Degradation kinetics revealed that ss-pLG notably degraded more compared to l-pLG scaffolds after 7 days of incubation in proteinase k and proteinase k+ lysozyme mixture containing PBS medium owing to their porosity and hydrophilicity nature. The mechanical strength of l-pLG was significantly higher than ss-pLG scaffolds because of the variable levels of gelatin grafting. Further, scaffolds of l-pLG and ss-pLG showed excellent compatibility to C2C12 and L929 cells. In addition, cell proliferation of C2C12 and L929 cells was found significantly more in l-pLG and ss-pLG scaffolds, respectively; which may be attributed to the strength compliance of scaffolds. Therefore, this modular approach of synthesizing functional polymer with tunable mechanical property can be used to fabricate 3D scaffolds for diverse cell and tissue engineering applications.